INTERNATIONAL JOURNAL FOR NUMERICAL METHODS IN FLUIDS
Int. J. Numer. Meth. Fluids 2006; **50**:397–420
Published online 23 August 2005 in Wiley InterScience (www.interscience.wiley.com). DOI: 10.1002/fld.1058

Swelling effect on the dynamic behaviour of composite cylindrical shells conveying fluid

M. H. Toorani[1,‡] and A. A. Lakis[2,*,†]

[1]*Nuclear Engineering Department, Babcock & Wilcox Canada, Cambridge, Ont., Canada*
[2]*Mechanical Engineering Department, Polytechnique of Montreal, Montreal, Que., Canada*

SUMMARY

This paper presents a semi-analytical investigation of a fluid–structure system. Both isotropic and composite cylindrical shells filled with or subjected to a flowing fluid have been considered in this study. The structure may be uniform or non-uniform in the circumferential direction. The hybrid finite element approach, shearable shell theory and velocity potential flow theory have been combined to establish the dynamic equations of the coupled system. The set of matrices describing their relative contributions to equilibrium is determined by *exact* analytical integration of the equilibrium equations. The linear potential flow theory is applied to describe the fluid effects that lead to the inertial, centrifugal and Coriolis forces. The axisymmetric, beam-like and shell modes of vibrations in both cases of uniform and non-uniform cylindrical shells are investigated. Fluid elastic stability of a structure subjected to a flowing fluid is also studied. This theory yields the high and the low eigenvalues and eigenmodes with comparably high accuracy. Reasonable agreement is found with other theories and experiments.

KEY WORDS: fluid–structure interactions; composite; cylindrical shells; flow-induced vibrations

1. INTRODUCTION

Fluid–structure interaction occurs across many complex systems of engineering disciplines, ranging from nuclear power plants and turbo-machinery components, naval and aerospace structures, and dam reservoir systems to flow in the blood vessels. The forces generated by violent fluid–structure contacts can be very high; they are stochastic in nature (i.e. boundary layer of a turbulent flow induces a random pressure field on the shell's wall) and thus difficult to describe. They do, however, often constitute the design loading for the structure.

*Correspondence to: A. A. Lakis, Section of Applied Mechanics, Mechanical Engineering Department, Ecole Polytechnique of Montreal, P.O. Box 6079, Station Centre-ville, Montreal, Que., Canada H3C 3A7.
†E-mail: aouni.lakis@meca.polymtl.ca
‡E-mail: nuclear@babcock.com

Received 8 November 2004
Revised 4 July 2005
Accepted 5 July 2005

Hydrodynamic pressures are generated by the vibrating structure, and these pressures will modify the structural deformation, which, in turn, will modify the hydrodynamic pressures that caused them. The problem is a tightly coupled elasto-dynamic problem in which the structure and the fluid form a single system. Solution of these problems is obviously complex and technically challenging.

Nuclear-plant reliability depends directly on its component performance. The higher heat-transfer performance of nuclear plant components often requires higher flow velocities through the shell and tube heat exchangers, which means these cylindrical structures are subjected to either axial or cross flow. The excessive flow-induced vibrations, which are a major cause of machinery downtime, fatigue failure and high noise, limit the performance of these structures. Therefore, the safety of a nuclear power plant's components requires an analysis of several possibilities of accident events. Considering a tube structure carrying high-velocity flow under high pressure, these events could be: pressure oscillations in a nuclear reactor cavity, velocity oscillations of a fluid in a pipe due to external excitations and fluid-elastic instabilities, among others.

These tubes could be subjected to diodic leak conditions (internal pressurization to point of tube yielding/swelling) that result in contact with their supports where there is a risk of structural degradation. Tube lock-up as a result of tube swelling due to diodic leakage could potentially result in tubes being locked at the supports and subject to wear. Locked supports will result in a loss of damping since the support damping is no longer active. The swelled tube would therefore be subjected to fluid-elastic instability.

There have been a significant number of experimental and analytical approaches to understanding the flow-induced instability mechanisms that occur in nuclear and heat exchanger components subjected to axial or cross-flow. The evaluation of the complex vibrational behaviour of these structures is therefore highly desirable in this sector of the industry. The review papers by Païdoussis [1], Pettigrew [2] and Chen [3] provide summaries of the progress made in developing design guidelines for both heat exchanger and nuclear components and the understanding of fluid-elastic excitation mechanisms. Weaver and Fitzpatrick [4] review the phenomenon of fluid-elastic instability in heat exchanger tube bundles under flow conditions. Païdoussis [5, 6] presents a dynamic study, both analytically and experimentally, of slender structures in contact with axial flow, in which the structure either contains the flow or is subjected to it—or both—and flow-induced instabilities have been thoroughly studied. Pettigrew [7] discusses relevant aspects of nuclear component vibration technology, namely, examples of vibration excitation mechanisms in axial flow, vibrations in two-phase flow, flow-induced vibration analysis and fretting-wear predictions. Seybert [8] uses the Ritz method along with a combination of finite-element and boundary-element methods to study fluid–structure interaction problems. Rajasankar *et al.* [9] present the results of investigations that evaluate the added mass to represent the fluid effect in 3-D problems. Au-Yang [10] provides practical information on the most common flow-induced vibration problems in power and process plant components. Blevins [11] presents some analytical tools for the vibration analysis of structures exposed to fluid flow. Different types of flow-induced vibrations are well classified and described. The effects of oscillatory flow, turbulence and sound on the structure as well as flow-induced sound (aeroacoustics) are also investigated.

The present theoretical investigation seeks a better understanding of: (1) the hydrodynamic pressure generated in the fluid because of the vibrational motion of the structure and (2) the effects of the fluid on the dynamic properties of the structure. The natural frequencies

and associated mode shapes are determined through a fully analytical approach for both the structure and the fluid domains. This paper examines cases where the fluid–structure interaction of composite cylindrical shells is characterized by the both external and internal fluid loading (inertial, Coriolis and stiffness loads due to flowing fluid). In the case of non-flowing fluid, the added mass effect of the fluid on the structure is often characterized as a low-frequency or long-time response. The structural deformation wavelengths cannot efficiently excite the long acoustic wavelengths (i.e. low frequency) associated with the structure's response frequencies. Therefore, the fluid behaves as nearly incompressible, as it flows back and forth across the wetted surface of the structure. The kinetic energy of the fluid coupled with the structure produces the added mass. Considering flowing fluid leads to inertia, Coriolis and centrifugal forces. In this work, the equations of the shell based on shearable shell theory are used to determine the pertinent displacement functions, instead of using the more common arbitrary polynomial forms. In doing so, the accuracy of the formulation is less affected as the number of elements used is decreased, thus reducing computation time. This formulation allows for convenient modelling in the case of circumferentially non-uniform shells.

2. BASIC THEORY AND STRUCTURE MODEL

The combination of the first-order transverse shear deformation theory of shells and the hybrid finite element method has been used to develop the dynamic equations of motion. The following assumptions have been made in the structural modelling:

(i) Use the linear elastic behaviour of laminated composite materials;
(ii) The shell is thin; it is therefore assumed that the normal thickness-direction stress is negligible compared with stress tangential to the shell surface;
(iii) Use the Green's exact strain–displacement relations that are expressed in arbitrary orthogonal curvilinear coordinates;
(iv) Adopt the first-order transverse shear deformation theory of the shells.

2.1. Kinematics

The shell is subdivided into finite segment panels (Figure 1(a)) with two nodal lines having five degrees of freedom at each node. The general strain–displacement relations are expressed in arbitrary orthogonal curvilinear coordinates to define the strain–displacement relations. The physical strain vector in the orthogonal curvilinear coordinate system is defined as follows:

$$\varepsilon_{ij} = \frac{\gamma_{ij}}{h_i h_j} \tag{1}$$

where γ_{ij} and h_i $(i = 1, 2, 3)$ are, respectively, the second rank symmetric tensor and the scale factors that are given in Reference [12]. For rigid body motion, the elongation γ_{ii} (no sum) and the shears γ_{ij} $(i \neq j)$ are identically zero, and there are therefore no theoretical limitations. The following kinematics relations are defined for the arbitrary shell described in orthogonal

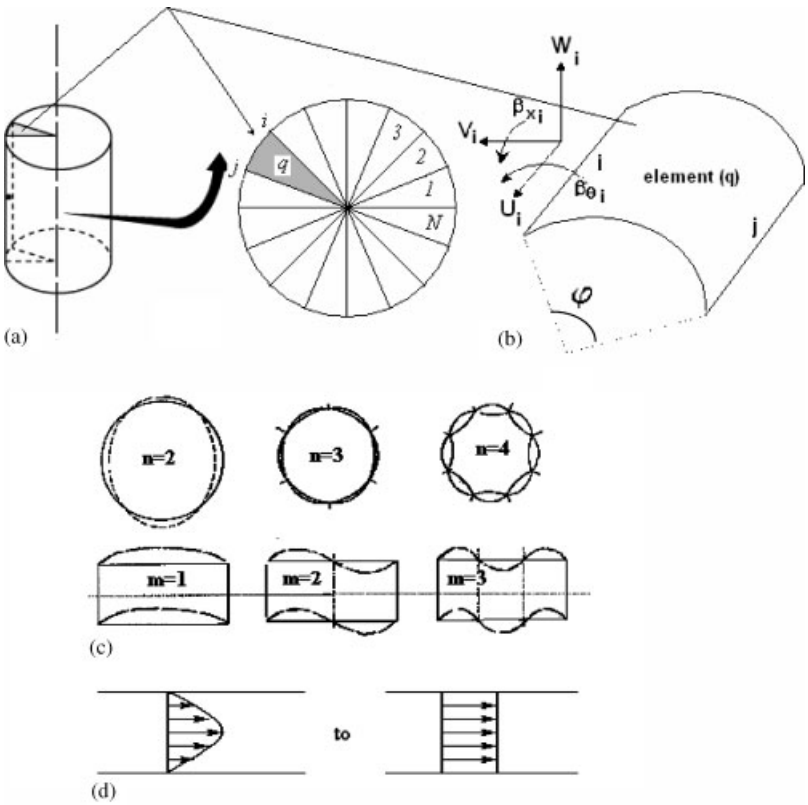

Figure 1. (a) Finite element discretization (N is the number of elements). (b) Nodal displacement at node 'i' of a typical element. (c) Circumferential and axial wave numbers, n and m, respectively. (d) Axial velocity.

curvilinear coordinates:

$$\begin{aligned} U(\alpha_1,\alpha_2,\xi) &= \left(1+\frac{\xi}{R_1}\right)u_x(\alpha_1,\alpha_2)+\xi\beta_x(\alpha_1,\alpha_2) \\ V(\alpha_1,\alpha_2,\xi) &= \left(1+\frac{\xi}{R_2}\right)u_\theta(\alpha_1,\alpha_2)+\xi\beta_\theta(\alpha_1,\alpha_2) \\ W(\alpha_1,\alpha_2,\xi) &= w(\alpha_1,\alpha_2) \end{aligned} \tag{2}$$

where the five degrees of freedom, u, v, w, β_x and β_θ are functions of the in-plane coordinates α_1 and α_2 in which u, v and w are, respectively, the axial, circumferential and radial displacements, and β_α $(\alpha = x, \theta)$ are rotations of the tangents to the reference surface oriented along parametric lines of mid-surface and ξ denotes the distance of the point from the corresponding point on the reference surface along the shell's thickness, and (R_1 and R_2) are the curvature radius. Substituting Equation (2) for Equation (1), the following strain–displacement

relations are obtained for cylindrical shells

$$\{\varepsilon\} = \{\varepsilon_x^0 \quad \gamma_x^0 \quad \mu_x^0 \quad \varepsilon_\theta^0 \quad \gamma_\theta^0 \quad \mu_\theta^0 \quad \kappa_x \quad \tau_x \quad \kappa_\theta \quad \tau_\theta\}^{\mathrm{T}} \tag{3}$$

where

$$\begin{aligned}
&\varepsilon_x^0 = \frac{\partial U}{\partial x}, \quad \gamma_x^0 = \frac{\partial V}{\partial x}, \quad \mu_x^0 = \frac{\partial W}{\partial x} + \beta_x \\
&\varepsilon_\theta^0 = \frac{1}{R}\frac{\partial V}{\partial \theta} + \frac{W}{R}, \quad \gamma_\theta^0 = \frac{1}{R}\frac{\partial U}{\partial \theta}, \quad \mu_\theta^0 = \frac{1}{R}\frac{\partial W}{\partial \theta} - \frac{V}{R} + \beta_\theta \\
&\kappa_x = \frac{\partial \beta_x}{\partial x}, \quad \tau_x = \frac{\partial \beta_\theta}{\partial x} + \frac{1}{2R}\frac{\partial V}{\partial x} \\
&\kappa_\theta = \frac{1}{R}\frac{\partial \beta_\theta}{\partial \theta}, \quad \tau_\theta = \frac{1}{R}\frac{\partial \beta_x}{\partial \theta} - \frac{1}{2R^2}\frac{\partial U}{\partial \theta}
\end{aligned} \tag{4}$$

here, $\varepsilon_j^0, \gamma_j^0, \kappa_j, \tau_j$ and μ_j^0 ($j = x/\text{or } \theta$) are normal and in-plane shearing strain, change in curvature, torsion of the reference surface and the shearing strain components, respectively (see Reference [13] for more details). U, V, W, β_x and β_θ are components of the displacement field.

2.2. Constitutive relations

The stress–strain relationship of the laminated composite cylindrical shells can be written as follows:

$$\{N_{xx} \quad N_{x\theta} \quad Q_{xx} \quad N_{\theta\theta} \quad N_{\theta x} \quad Q_{\theta\theta} \quad M_{xx} \quad M_{x\theta} \quad M_{\theta\theta} \quad M_{\theta x}\}^{\mathrm{T}} = [P]\{\varepsilon\}^{\mathrm{T}} \tag{5}$$

It is observed that the symmetry of the stress tensor does not necessarily imply that $N_{x\theta}$ and $N_{\theta x}$ or $M_{x\theta}$ and $M_{\theta x}$ are equal except in the case of a spherical shell, a flat plate or a thin shell of any shape. The elasticity matrix $[P]$ given in Reference [13] can be applied to shells consisting of a single or an arbitrary number of isotropic, quasi-isotropic and orthotropic layers. In the case of an arbitrary number of orthotropic layers, we assume that these layers function concurrently without slippage.

2.3. The equations of motion

The virtual displacement principle is applied to obtain the equations of motion for the anisotropic circular cylindrical shells that are fully given in Reference [13]. These governing equations have been developed in terms of displacement measures. Therefore, the five independent boundary conditions must be specified on each edge of the shell, Figure 1(b). The transverse shear deformations do not disappear in this theory and, therefore, the β_i cannot be expressed in terms of U_i and W. The transverse shear theory recommended here leads to no strains during rigid body motion.

2.4. The displacement functions

The displacement components U, V, W, β_x and β_θ of the mean surface of the shell are expressed by

$$\begin{Bmatrix} U_x(x,\theta) \\ U_\theta(x,\theta) \\ W(x,\theta) \\ \beta_x(x,\theta) \\ \beta_\theta(x,\theta) \end{Bmatrix} = \sum_{i=1}^{10} \begin{bmatrix} \mathrm{Cos}\,\bar{m}x & 0 & 0 & 0 & 0 \\ 0 & \mathrm{Sin}\,\bar{m}x & 0 & 0 & 0 \\ 0 & 0 & \mathrm{Sin}\,\bar{m}x & 0 & 0 \\ 0 & 0 & 0 & \mathrm{Cos}\,\bar{m}x & 0 \\ 0 & 0 & 0 & 0 & \mathrm{Sin}\,\bar{m}x \end{bmatrix} \begin{Bmatrix} A_i \mathrm{e}^{\eta_i \theta} \\ B_i \mathrm{e}^{\eta_i \theta} \\ C_i \mathrm{e}^{\eta_i \theta} \\ D_i \mathrm{e}^{\eta_i \theta} \\ E_i \mathrm{e}^{\eta_i \theta} \end{Bmatrix} \tag{6}$$

where $\bar{m} = m\pi/L$, m is the axial wave number, L is the shell's length, η_i are complex roots of the characteristic equation (7). These η_i represent the circumferential wave number in Equation (6). For each 'm', the solution of the dynamic equation (12) developed in the next section, will lead to the shapes (η_i) of the circumferential wave number 'n'. A closed cylinder or any other shell undergoing vibrations may be deformed in a variety of ways, as shown in Figure 1(c) where several configurations are given. Viewed from one end, the vibration of the shell may consist of any number of waves distributed around the circumference. Denoting the number of these waves by n, we see, in Figure 1(c), cases of n equal to 2, 3, and 4. When, viewed from its side, the deformation of the cylinder consists of a number of waves distributed along the length of a generator. We obtain, for example, for $n = 4$, eight circumferential half-waves.

Substituting Equation (5) into the differential equations of motion yields the five linear differential operators L_i. The implicit forms of these equations, in which the shear deformation effects and inertia terms are included, are defined as follows (see Reference [13] for full length equations).

$$L_q(u_x, u_\theta, w, \beta_x, \beta_\theta, P_{ij}) = 0; \quad q = 1, \ldots, 5 \text{ and } i, j = 1, 2, \ldots, 10 \tag{7}$$

Substituting Equation (6) into Equation (7) and considering the non-trivial solution leads to a tenth-order characteristic equation

$$\mathrm{Det}([H]) = f_{10}\eta^{10} + f_8\eta^8 + f_6\eta^6 + f_4\eta^4 + f_2\eta^2 + f_0 = 0 \tag{8}$$

where f_i ($i = 0$–10) are coefficients of the determinant of the equations of motion $[H]$ whose elements are given in Appendix A. Each root of this equation yields a solution to the equations of motion. The complete solution is obtained by the sum of all 10 independent solutions. The five equations of motion are implicit relations among the 10 resultant forces and moments. Therefore, the five necessary boundary conditions must be specified on each edge of the shell. It should be noted that these governing equations are expressed in terms of displacement measure only, named the Dirichlet (essential) boundary value problem. The degrees of freedom at nodal line i (Figure 1(b)) can be defined by the following vector:

$$\{\delta_i\} = \{u_{x_i} \quad u_{\theta_i} \quad w \quad \beta_{x_i} \quad \beta_{\theta_i}\}^{\mathrm{T}} \tag{9}$$

Each element has two nodal lines (Figure 1(b)) and 10 degrees of freedom, and θ has a definite value ($\theta = 0$ at node i) and ($\theta = \varphi$ at node j), so the following relation can present the element displacements at the boundaries:

$$\begin{Bmatrix} U_x(x,\theta) \\ U_\theta(x,\theta) \\ W(x,\theta) \\ \beta_x(x,\theta) \\ \beta_\theta(x,\theta) \end{Bmatrix} = [N] \begin{Bmatrix} \delta_i \\ \delta_j \end{Bmatrix} \tag{10}$$

These equations determine the displacement functions.

2.5. *Determination of mass and stiffness matrices for an element*

The mass and stiffness matrices for one element can be expressed as

$$\begin{aligned} [m] &= \rho h \int_0^{\mathrm{L}} \int_0^{\varphi} [N]^{\mathrm{T}}[N] R \, \mathrm{d}x \, \mathrm{d}\theta = \rho h [A^{-1}]^{\mathrm{T}}[S][A^{-1}] \\ [k] &= \int_0^{\mathrm{L}} \int_0^{\varphi} [B]^{\mathrm{T}}[\mathrm{P}][B] R \, \mathrm{d}x \, \mathrm{d}\theta = [A^{-1}]^{\mathrm{T}}[G][A^{-1}] \end{aligned} \tag{11}$$

where ρ is the density of the shell, h and R are the thickness and the shell's radius, respectively.

The $[G]$ and $[S]$ matrices are developed analytically by carrying out the necessary matrix operations and analytical integration over x and θ in Equation (11). These matrices ($[A], [G]$ and $[S]$) are given in terms of shell's characteristics, material properties, η_i, and the axial wave number m.

3. FREE VIBRATION

As previously stated, the complete shell is subdivided into finite elements. Each element is made of cylindrical panel segments with two nodal lines, Figure 1(b). The global mass $[M]$ and stiffness $[K]$ matrices for the whole structure can be constructed whenever the mass $[m]$ and stiffness matrices $[k]$ of all elements are obtained. For free vibration, the equations of motion may be written in the form

$$[M]\{\ddot{\Delta}\} + [K]\{\Delta\} = 0 \tag{12}$$

where $[\Delta] = \{\delta_1, \delta_2, \ldots, \delta_{N+1}\}^{\mathrm{T}}$, N is the number of elements, $[M]$ and $[K]$ are real, symmetric matrices of order $5(N+1) \times 5(N+1)$, and $\{\delta_{N+1}\}$ is the displacement vector associated with the lower edge of the last element. In the case where the shell has rigid edge constraints, the kinematics boundary conditions must be taken into account. Accordingly, $[K]$ and $[M]$ are reduced to square matrices of order $5(N+1) - J$, where J is the number of the constraint equations imposed.

The solution of Equation (12) now follows by standard matrix techniques, yielding the natural frequencies, $\omega_i i = 1, 2, \ldots, 5(N+1) - J$ and the corresponding eigenvectors. It must be stressed that the mass and stiffness matrices, eigenvalues and shape modes obtained are associated with a specific axial wave number, m. It means that the analysis is thus performed independently for each m.

4. THE FLUID MODEL

A finite fluid element bounded by two nodal lines, Figure 1(b), is considered to account the effect of the fluid on the structure. It is assumed that the shell is subjected only to a potential flow that leads to the inertial, centrifugal and Coriolis forces to participate in the flow-induced vibration pattern. The mathematical model is based on the following hypothesis: (i) the fluid flow is potential; (ii) the fluid is irrotational, incompressible and non-viscous; (iii) the deformations are small, allowing the use of linear theory; (iv) the axial fluid mean velocity distribution, U_x, is assumed to be constant across a shell section (See Figure 1(d)).

4.1. Dynamic pressure

The velocity function for ideal frictionless flow in the linear form must satisfy the following equation for a non-viscous fluid:

$$\left\{ \frac{1}{C_f^2} \left[\frac{\partial^2(\,)}{\partial t^2} + 2U_x \frac{\partial^2(\,)}{\partial x \partial t} + U_x^2 \frac{\partial^2(\,)}{\partial x^2} \right] - \nabla^2 \right\} \phi = 0 \tag{13}$$

where C_f is the speed of sound in the fluid, t is the time variable, U_x is the axial velocity of the fluid through the shell section, ϕ is the potential function and ∇^2 is the Laplace operator in cylindrical coordinates. Assuming an incompressible fluid ($C_f = 0$), Equation (13) becomes Laplace's equation which is expressed in the cylindrical coordinate system by

$$\frac{1}{r} \frac{\partial}{\partial r} \left(r \frac{\partial \phi}{\partial r} \right) + \frac{1}{r^2} \frac{\partial^2 \phi}{\partial \theta^2} + \frac{\partial^2 \phi}{\partial x^2} = 0 \tag{14}$$

where ϕ is the potential function.

The flow velocity in case of potential flow theory is expressed as follows:

$$V = \nabla \phi + U_x \tag{15}$$

where $\nabla \phi$ is the unsteady part of velocity, which may be obtained from a velocity potential, and U_x is the mean flow velocity. Therefore, the components of the flow velocity are given by

$$V_x = U_x + \frac{\partial \phi}{\partial x}, \quad V_\theta = \frac{1}{R} \frac{\partial \phi}{\partial \theta}, \quad V_r = \frac{\partial \phi}{\partial r} \tag{16}$$

where V_x, V_θ and V_r are, respectively, the axial, tangential and radial components of the fluid velocity, U_x is the velocity of the liquid through the shell section. The Bernoulli equation is given by

$$\left(\frac{\partial \phi}{\partial t} + \frac{V^2}{2} + \frac{P}{\rho_f} \right) \Bigg|_{r=R} = 0 \tag{17}$$

Substituting for V^2 ($V^2 = V_x^2 + V_\theta^2 + V_r^2$), the dynamic pressure '$P(x,r,\theta,t)$', exerted on the shell's wall, can be found as

$$P_{\mathrm{i,e}} = -\rho_{\mathrm{f_{i,e}}}\left(\frac{\partial\phi_{\mathrm{i,e}}}{\partial t} + U_{x_{\mathrm{i,e}}}\frac{\partial\phi_{\mathrm{i,e}}}{\partial x} + \frac{U_{x_{\mathrm{i,e}}}^2}{2} + \frac{1}{2}\left[\left(\frac{\partial\phi_{\mathrm{i,e}}}{\partial x}\right)^2 + \frac{1}{r^2}\left(\frac{\partial\phi_{\mathrm{i,e}}}{\partial\theta}\right)^2 + \left(\frac{\partial\phi_{\mathrm{i,e}}}{\partial r}\right)^2\right]\right)_{r=R_{\mathrm{i,e}}=R\mp t/2} \tag{18}$$

The present theory is equally valid for internal and external flows, therefore the subscripts 'i' and 'e' in Equation (18) denote the '*internal*' and '*external*' fluid, respectively. In the present theory, only the two first terms appeared at the right-hand side of Equation (18) are taken into account, the third term is a constant and the other terms are non-linear terms.

A full definition of the flow requires that the boundary conditions applied on the shell–fluid interface are specified. Therefore, the boundary condition at fluid–shell surface is defined as follows:

At the $r = R$, the radial velocity of the fluid should match the instantaneous rate of change of the shell displacement in the radial direction (the impermeability condition). This condition implies a permanent contact between the shell surface and the peripheral fluid layer, which should be

$$V_r|_{r=R} = \left.\frac{\partial\phi}{\partial r}\right|_{r=R} = \left(\frac{\partial W}{\partial t} + U_x\frac{\partial W}{\partial x}\right)_{r=R} \tag{19}$$

Assuming compatibility between the motion of the shells' wall and fluid, the radial displacement, from shell theory, is defined as (see Equation (6))

$$W(x,\theta,t) = \sum_{j=1}^{10} C_j \exp[\eta_j\theta + \mathrm{i}\omega t]\sin(\bar{\mathrm{m}}x) \tag{20}$$

where η_j is the jth root of the characteristic equation (8), ω is the natural angular frequency and t is time variable. The differential equation (14) can be solved using the separation of variables method. The velocity potential is assumed to be

$$\phi(x,\theta,r,t) = \sum_{j=1}^{10} R_j(r)S_j(x,\theta,t) \tag{21}$$

The function $S_j(x,\theta,t)$ can be explicitly determined after applying the impermeability condition (19) and using the radial displacement relation given by Equation (20). Substituting the explicit term of $S_j(x,\theta,t)$ into Equation (21), we obtain

$$\phi(x,\theta,r,t) = \sum_{j=1}^{10}\frac{R_j(r)}{(\partial R_j(R)/\partial r)}\left[\frac{\partial W_j}{\partial t} + U_x\frac{\partial W_j}{\partial x}\right] \tag{22}$$

Introducing this explicit term (22) and Equation (20) into Equation (14), we obtain Bessel's homogeneous differential equation.

$$r^2 \frac{\mathrm{d}^2 R_j(r)}{\mathrm{d}r^2} + r \frac{\mathrm{d}R_j(r)}{\mathrm{d}r} + R_j(r)[i^2 \Xi_j^2 r^2 - (i\eta_j)^2] = 0 \tag{23}$$

where 'i' is the complex number, $i^2 = -1$ and Ξ_j is defined as follows:

$$\Xi_j^2 = \begin{cases} \left(\dfrac{m\pi}{L}\right)^2 & \text{if } 1/C_\mathrm{f} = 0 \text{ (incompressible fluid)} \\ \left(\dfrac{m\pi}{L}\right)^2 - \dfrac{1}{C_\mathrm{f}^2}\left(\omega - \mathrm{i}U_x \dfrac{m\pi}{L}\right)^2 & \text{if } 1/C_\mathrm{f} \neq 0 \end{cases} \tag{24}$$

where η_j, R, ω and U_x are the roots of the characteristic equation (8), the radius of the shell, the natural angular frequency and the axial flow velocity, respectively. The general solution of Equation (23) is given by

$$R_j(r) = AJ_{i\eta_j}(i\Xi_j r) + BY_{i\eta_j}(i\Xi_j r) \tag{25}$$

where J_{nj} and Y_{nj} are Bessel functions of the first and second kind of order n, respectively. For a shell filled with a liquid (internal flow), the constant 'B' must be set equal to zero, since the Y_{nj} is singular at $r = 0$. For a shell submerged in a liquid (external flow), the constant 'A' is equal to zero. The complete solution is found when the shell is simultaneously subjected to internal and external flow.

An expression for dynamic pressure as a function of the displacement W_j and the function $R_j(r)$, taking into account only the linear terms, is obtained by substituting Equation (22) and the first derivation of the Bessel function, of the first and second kind, into Equation (18)

$$P_\mathrm{u} = -\rho_\mathrm{u} \sum_{j=1}^{10} Z_{ij}(i\Xi_k R_\mathrm{u}) \left[\frac{\partial^2 W_j}{\partial t^2} + 2U_{x_\mathrm{u}} \frac{\partial^2 W_j}{\partial x \partial t} + U_{x_\mathrm{u}}^2 \frac{\partial^2 W_j}{\partial x^2}\right] \tag{26}$$

where subscript 'u' indicates 'i' or 'e', which denote the internal or external fluid (the present theory is equally valid for internal and external flows), and $\rho_{\mathrm{e,i}}$ is the density of external or internal fluid and

$$Z_{ij}(i\Xi_k R_i) = \frac{R_i}{i\eta_j - i\Xi_k R_i \dfrac{I_i \eta_{j+1}(i\Xi_k R_i)}{I_i \eta_j (i\Xi_k R_i)}} \tag{27}$$

where

$$R_i = \begin{cases} R - t/2 \\ R + t/2 \end{cases} \quad \text{and} \quad I_i = \begin{cases} J_i & \text{Case of Internal flow} \\ Y_i & \text{Case of External flow} \end{cases}$$

Introducing the displacement function (20) into the dynamic pressure expression in (26) and carrying out the necessary matrix operations, the mass, damping and stiffness matrices for the fluid are obtained by integrating the following equation with respect to x and θ:

$$\{F\} = \int_A [N]^\mathrm{T} \{P_\mathrm{u}\} \, \mathrm{d}A \tag{28}$$

In Equation (26) the given terms in bracket indicate the inertia, centrifuge and Coriolis forces, respectively, due to flowing fluid. These forces that are obtained analytically, by integrating Equation (28), which may be rewritten as follows:

$$\begin{aligned}[m_f] &= [A_f^{-1}]^T[S_f][A_f^{-1}] \\ [c_f] &= [A_f^{-1}]^T[D_f][A_f^{-1}] \\ [k_f] &= [A_f^{-1}]^T[G_f][A_f^{-1}]\end{aligned} \tag{29}$$

The matrix $[A]$ is defined by Equation (11) and the elements of $[S_f], [D_f]$ and $[G_f]$ matrices are given in Appendix A.

The Coriolis force, $[c_f]$, results from the coupling of the relative velocity of the fluid with the rotation of a section of the structure. It is important to note that the centrifugal and Coriolis terms have a special importance here, since they are responsible for the non-conservative aspects of the problems to be solved. Mathematically, they cause the differential equations that generate complex eigenvalue problems. Physically, the system experiences static (buckling) and dynamic (flutter) instability.

5. COUPLED FLUID–STRUCTURE MODEL

The structural and fluid mass and stiffness matrices as well as the fluid damping matrix, given in the previous sections, are only determined for one element. The overall mass, stiffness and damping matrices are obtained by assembling the matrices for each element. Assembling is done in such a way that all the equations of motion and the continuity of displacements at each node are satisfied. These matrices are designated as $[M]$, $[K]$ and $[C]$, respectively.

$$([M_s] - [M_f])\{\ddot{\delta}\} - [C_f]\{\dot{\delta}\} + ([K_s] - [K_f])\{\delta\} = \{0\} \tag{30}$$

where $\{\delta\}$ is the displacement vector and $[M_s]$ and $[K_s]$ are the mass and stiffness matrices of the structure, respectively, and $[M_f]$, $[K_f]$ and $[C_f]$ are the inertial, centrifugal and Coriolis forces, respectively, due to the fluid effect. The global dynamic equations of the coupled system are defined as

$$\begin{bmatrix} [0] & \dfrac{[M]}{\omega_0} \\ \dfrac{[M]}{\omega_0^2} & \dfrac{[C]}{\omega_0} \end{bmatrix} \begin{Bmatrix} \ddot{\delta} \\ \dot{\delta} \end{Bmatrix} + \begin{bmatrix} -\dfrac{[M]}{\omega_0} & [0] \\ [0] & [K] \end{bmatrix} \begin{Bmatrix} \dot{\delta} \\ \delta \end{Bmatrix} = 0 \tag{31}$$

where $\omega_0 = p_{11}$ is the first element of the elasticity matrix and $M = M_s - M_f$; $K = K_s - K_f$ and $C = C_f$.

The eigenvalue problem is expressed as

$$|[DD] - \Lambda[I]| = 0 \tag{32}$$

where

$$[DD] = \begin{bmatrix} [0] & [I] \\ -\frac{1}{\omega_0^2}[K]^{-1}[M] & -\frac{1}{\omega_0}[K]^{-1}[C] \end{bmatrix} \tag{33}$$

and $\Lambda = 1/\omega_0^2\omega^2$; ω is the radian natural frequency of the system. In the case of a non-flowing fluid ($U_x = 0$), the matrices $[K_f]$ and $[C_f]$ are not involved in the computations. The eigenvalue problem in this particular case is reduced to

$$|\omega_0^2[K]^{-1}[M] - \Lambda[I]| = 0 \tag{34}$$

6. CALCULATIONS AND DISCUSSION

To illustrate the versatility of the theory, numerical results concerned with the vibration and stability of cylindrical tubes subjected to both stationary and flowing fluid are presented. The proposed method is applied to obtain the natural frequencies of anisotropic and isotropic open and closed cylindrical shells that are empty, filled with or subjected to a flowing fluid. The axisymmetric, beam-like and shell mode behaviours of shells are studied. The values of the shear correction factors used in calculations have been taken as $\pi^2/12$. It should be noted that the authors also provide results using Sanders' theory [14] in some cases, for sake of comparison, using the present work where the transverse shear deformation effects are discarded. The following non-dimensional frequency parameters are used to present the numerical results:

$$\Omega = \omega R\sqrt{\rho_s(1-\nu^2)/E} \quad \text{for isotropic materials}$$

$$\Omega = (\omega R^2/h)\sqrt{\rho_s/E_2} \quad \text{for anisotropic materials}$$

$$\Omega = \omega/\omega_0 \quad \text{in case of stability analysis}$$

where ω is the natural frequency, $\omega_0 = p_{11}$ is the first element of the elasticity matrix, h is the shell thickness, ρ_s is structural density, E and E_2 are the modulus of elasticity.

The first set of calculations (Figure 2) deals with the non-dimensional fundamental frequencies of a simply supported cylindrical shell ($W(x,\theta,t) = V(x,\theta,t) = 0$). The shell is constituted of four symmetric cross-ply layered ($0^\circ/90^\circ/90^\circ/0^\circ$). All layers are assumed to be of the same geometric and material parameters and the individual layer is assumed to be orthotropic. The following material properties are used (the same properties are used hereafter for those structures that are made of composite materials)

$$E_1 = 25E_2; G_{23} = 0.2E_2; G_{13} = G_{12}, = 0.5E_2; \nu_{12} = 0.25; \rho = 1 \text{ (density)}$$

It is noted that the value of ρ is arbitrary because of the non-dimensionalization used. Therefore it is set to unity. The effects of the axial mode and radius-to-thickness ratio on the non-dimensional natural frequencies of multi-layered anisotropic cylindrical shell is shown in Figure 2. For the sake of comparison, the authors also provide some results

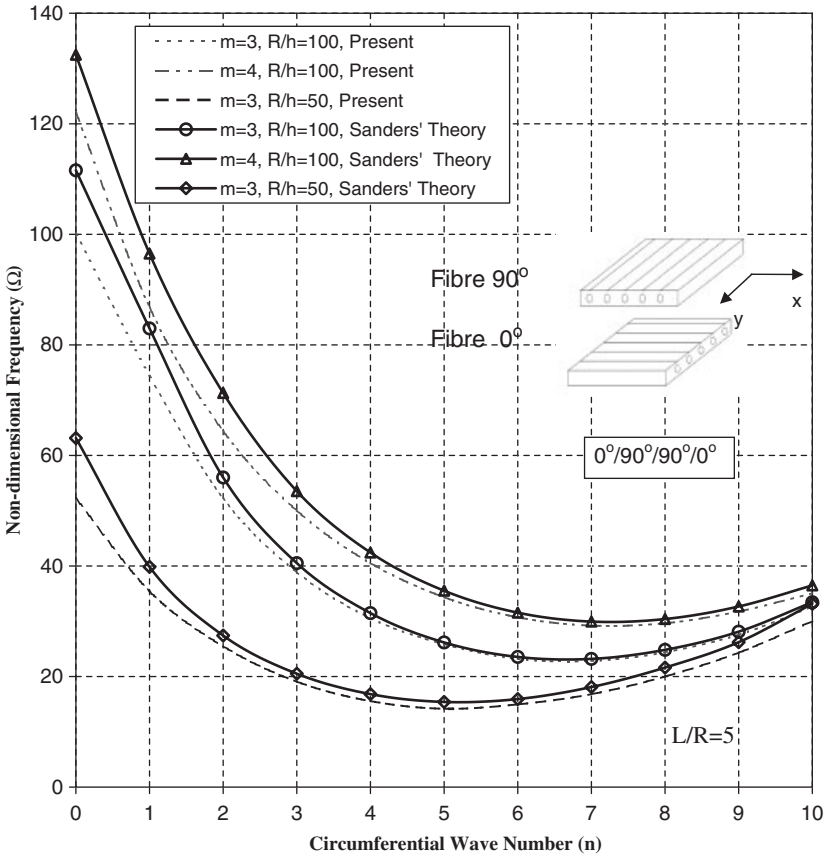

Figure 2. Non-dimensional frequency ($\Omega = (\omega R^2/h)\sqrt{\rho_s/E_2}$) distribution of a composite cylindrical shell.

based on Sanders' theory (neglecting shear deformation effects). This figure shows that the shear deformation has a more significant effect on the vibration characteristics of composite structures.

In Figure 3, we see the behaviour of an open cylindrical shell, empty or filled with liquid, as a function of the number of circumferential modes. For a given axial wave number '*m*' the frequencies decrease to minimum before they increase as the number of circumferential waves '*n*' is increased. This behaviour was first observed for a shell *in vacuo* by Arnold and Warburton [15] who were able to explain it by a consideration of the strain energy associated with bending and stretching of the reference surface. It may be concluded from their work, that at low '*n*' the bending strain energy is low and the stretching strain energy is high, while at the higher '*n*' the relative contributions from the two types of strain energy are reversed. The interchange in the relative contributions of the bending and stretching strain energy as the circumferential wave number '*n*' is increased explains the decrease and subsequent increase in the natural frequencies indicated in Figure 3. An open cylindrical shell partially or completely filled with liquid will behave in the same way.

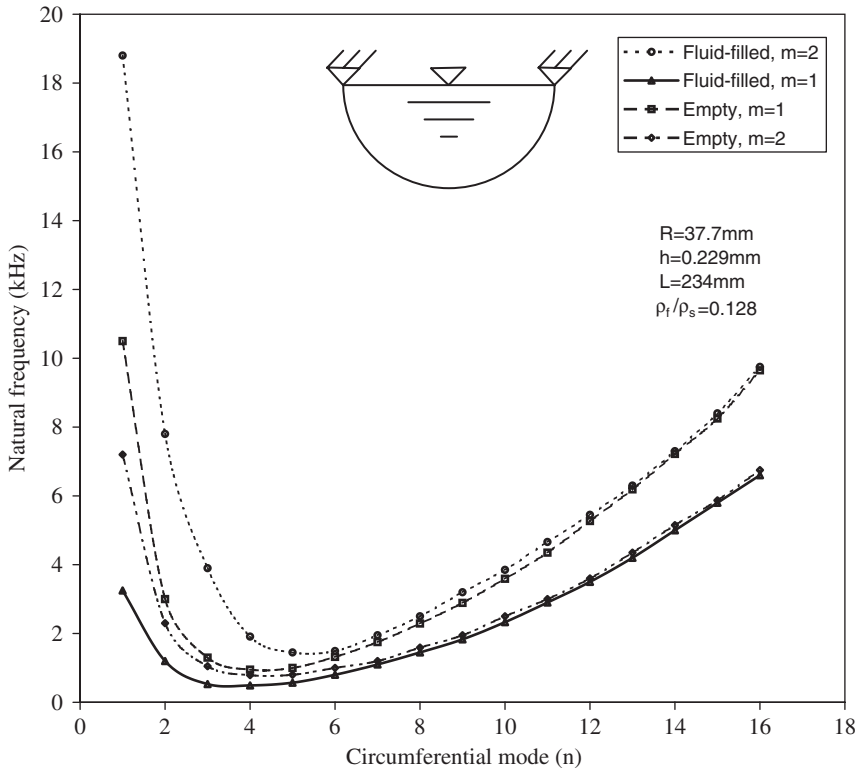

Figure 3. Natural frequency of an empty and fluid-filled open cylindrical shell as a function of circumferential mode number (n).

Table I. Natural frequencies (Hz) of simply supported isotropic shell; experimental data are from References [16, 17]. $R = 0.175$ m, $L = 0.664$ m, $E = 206$ GPa, $\nu = 0.3$, $\rho = 7680$ kg/m^3.

	n	2	3	4	5	6	7	8	9	10
$m = 1$	Empty	600.1	313.3	220.1	227.7	293.6	390.2	507.9	643.8	797.6
	Full	186.0	110.0	87.0	96.1	135.5	190.1	263.3	354.3	460.8
	Half-filled	337.4	177.4	93.1	120.3	222.8	274.0	372.3	488.5	618.1
	Experiment [18]	—	315	220	229	294	391	507	—	—
$m = 2$	Empty	1752.9	1035.4	671.2	493.4	438.59	468.9	554.9	676.2	822.9
	Full	572.8	377.6	270.8	208.6	199.3	229.9	278.5	361.9	461.3
	Half-filled	1011.6	610.5	469.9	309.4	205.2	234.1	390.9	511.1	648.3
	Experiment [18]	—	—	668	490	441	469	553	—	—

Table I presents the natural frequencies computed for a simply supported cylindrical shell. Dimensions and material properties are given in the caption of the table and correspond to the experiments performed by Amabili *et al.* [16, 17] on a stainless steel shell *in vacuo*. The

agreement between the present theoretical results and experimental data is excellent. Table II presents the non-dimensional frequency parameters of an anisotropic empty shell (having symmetric $0°/90°/90°/0°$ layout) in the case of axisymmetric mode ($n = 0$) as a function of the radius-to-thickness ratio and axial mode number.

Figure 4 shows the numerical results for an isotropic fluid-filled cylindrical shell for different values of L/R and R/t ratios. The fluid contained in the shell is water. Comparing the results obtained based on the present theory with those of classical shell theory (CST)

Table II. Non-dimensional natural frequency parameter ($\Omega = (\omega R^2/h)\sqrt{\rho_s/E_2}$) of a symmetric ($0°/90°/90°/0°$) cylindrical shell ($n = 0$ '*axi-symmetric mode*', *empty*, $L/R = 5$).

	m			
R/t	1	3	4	7
10	4.40	13.44	18.02	21.77
20	8.88	21.81	26.23	35.47
50	22.23	67.00	89.53	121.24
100	44.47	100.15	122.13	132.67

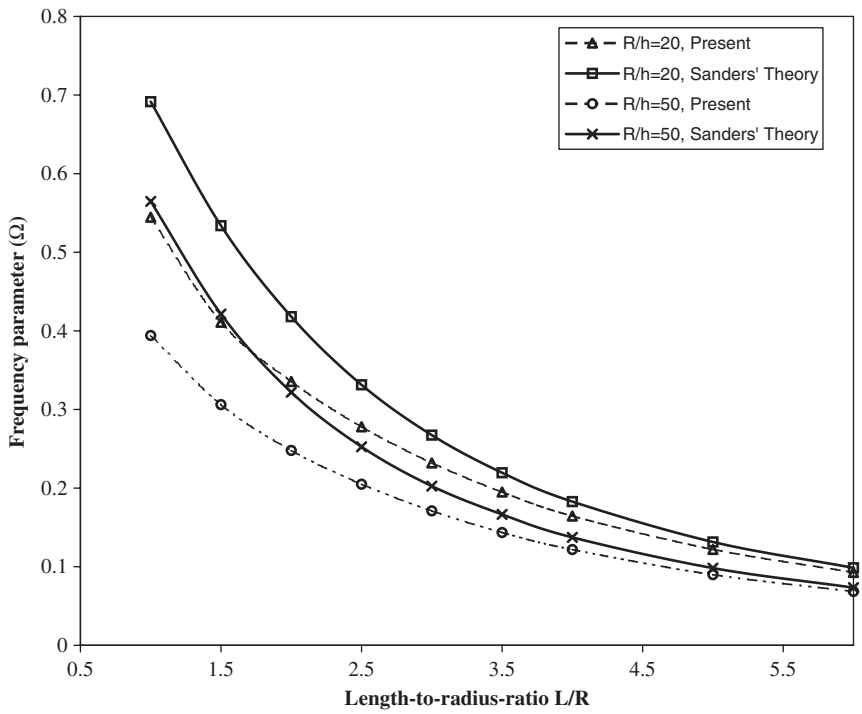

Figure 4. Variation of non-dimensional frequency ($\Omega = \omega R\sqrt{\rho_s(1 - \nu^2)/E}$) of a cylindrical shell.

shows a significant difference for low values of R/t and L/R ratios. This means that the shear deformation effects are more pronounced for thicker and shorted shells.

Figure 5 is drawn to show the shear deformation effects on the non-dimensional natural frequencies of fluid-filled cylindrical shells for different ratios of L/R and R/t along with the corresponding results based on Sanders' theory that are obtained by author by discarding the shear deformation effect in the present theory. It is observed that the classical shell theories overestimate the frequencies for all parameters considered.

The stability of shells subjected to a flowing fluid is of practical importance because the natural frequency of structures generally decreases with the increasing velocity of fluid flow. The decrease in natural frequency can be important in certain problems involving high-velocity flows through or crossing over the thin-walled structures such as those used in the feed lines to rocket motors, water turbines and nuclear steam generators. These structures may become susceptible to resonance or fatigue failure if their vibration frequency falls below certain limits. The non-dimensional parameters of velocity and frequency used for stability analysis are $U = U_x/u_0$ and $\Omega = \omega/\omega_0$, where

$$\omega_0 = \frac{\pi^2}{L^2}\left(\frac{K}{\rho_s h}\right)^{1/2}, \quad u_0 = \frac{\pi^2}{L}\left(\frac{K}{\rho_s h}\right)^{1/2}, \quad K = \frac{Eh^3}{12(1-\nu^2)}$$

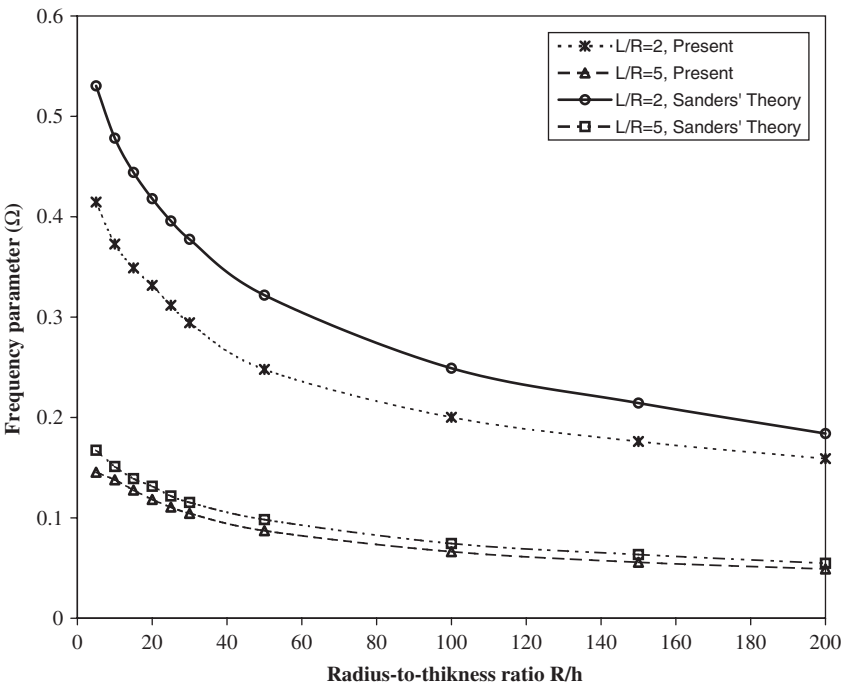

Figure 5. Frequency parameter ($\Omega = \omega R\sqrt{\rho_s(1-\nu^2)/E}$) of a fluid-filled cylindrical shell with respect to variation of R/h.

The influence of the flow velocity on the frequency parameter of cylindrical shells is studied through Figure 6 ($L/R=2$; $R/h=100$; $\rho_f/\rho_s=0.128$ and $n=5$). The first frequency becomes negative imaginary at $U=2.96$, indicating static divergence instability in the first axial mode, and reappeared and coalesced at $U=3.36$ with that of the second axial mode to produce mode flutter. As long as the effective stiffness of the system remains positive as flow velocity increases, the system will oscillate asymptotically about its neutral equilibrium position; otherwise, it will diverge to a new equilibrium position, different from neutral (buckling). As long as the effective fluid-damping of the system remains positive as flow velocity is increased, vibrations will be damped; otherwise, they will be amplified (flutter).

Figure 7 shows the divergence instability phenomena for an isotropic simply supported cylindrical shell ($L/R=2$; $R/h=100$ and $\rho_f/\rho_s=0.128$). Again, it is observed that the frequencies associated with all modes decrease as the flow velocity increases from zero. The frequency parameters remain real (the system being conservative) until they vanish at high velocities, indicating the existence of static divergence instability. In this case, the frequencies become purely imaginary. This figure shows that the dimensionless critical flow velocity increases, as the axial mode number is increased and the circumferential mode number decreased. If the velocity is further increased, the natural frequencies for all cases reappear and would coalesce with those of the following mode numbers to produce coupled mode flutter.

The frequency variation of an immersed cylindrical shell in the fluid media is depicted in Figure 8, as a function of the circumferential wave number. The obtained results are compared with those of Reference [19]. Physical and geometrical parameters are given along with the figure. The two theories give nearly identical results.

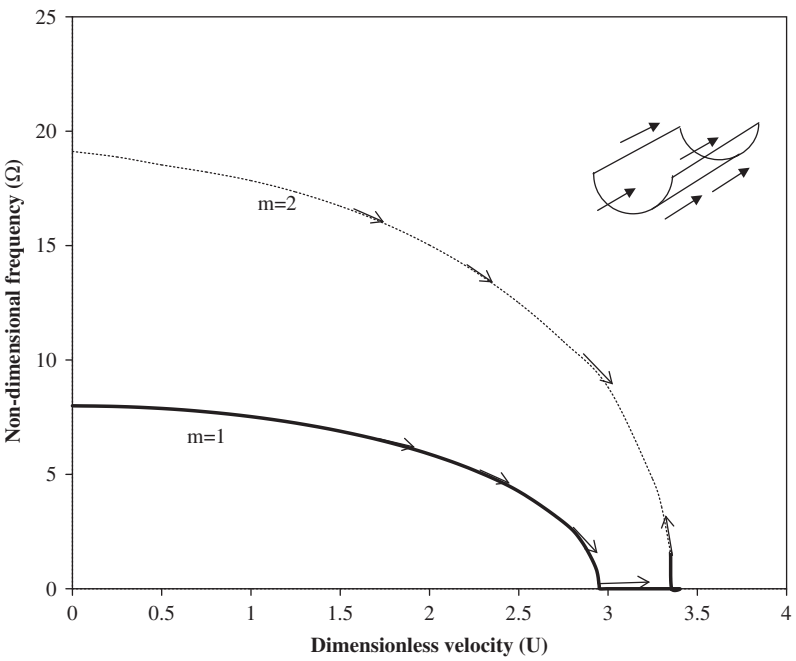

Figure 6. Stability of a cylindrical shell as a function of internal flow velocity.

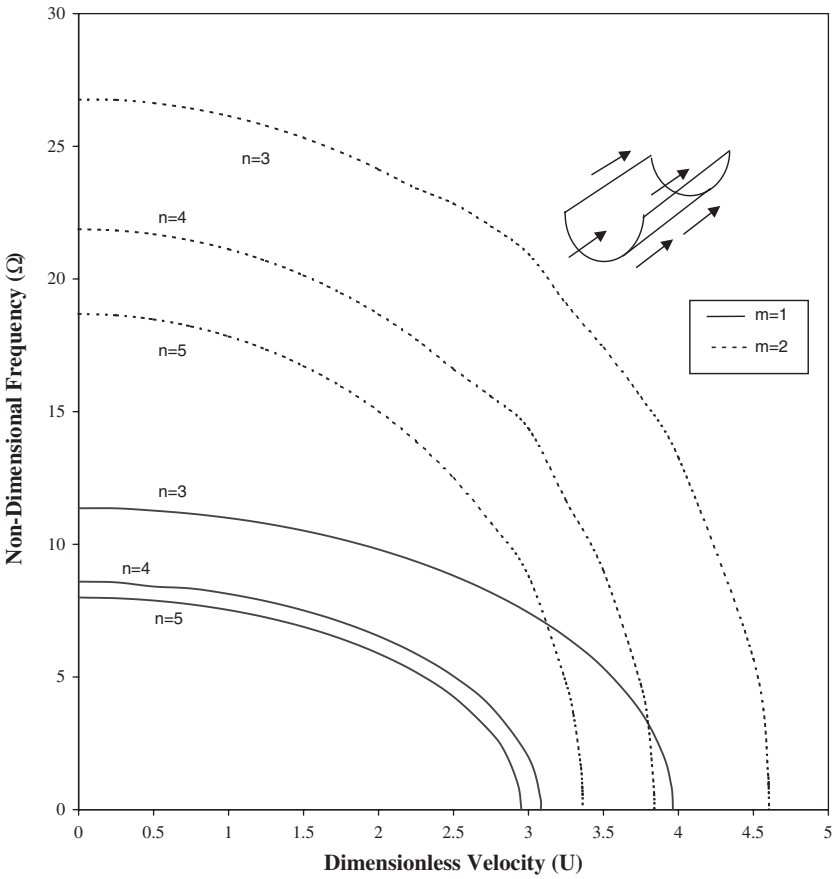

Figure 7. Stability of a cylindrical shell with respect to flow velocity.

The next example demonstrates the capability of the present method to calculate the natural frequencies of shells having circumferentially varying thicknesses: an isotropic cylinder whose inner bore is circular but non-concentric with circular outer surface. This case was studied by Tonin and Bies [18] using Rayleigh–Ritz method. The effect of the eccentricity on the calculated natural frequencies for various modes is detailed in Table III. The steel cylinder is free simply supported at both ends. The experimental results of Reference [18] are also given for sake of comparison with those of theoretical approaches. The results show that the effect of increasing eccentricity is to lower the frequencies of the shell.

The last example, Figure 9, is the stability analysis of a distorted cylindrical shell simply supported at both ends that is subjected to an internal flow. The natural frequencies of the system are examined as a function of the flow velocity. As the velocity increases from zero, the frequencies associated with all eccentricity cases decrease. They remain real (the system being conservative) until at sufficiently high velocities, they vanish, indicating the existence of buckling type (static divergence) instability. At higher flow velocity, the frequencies become

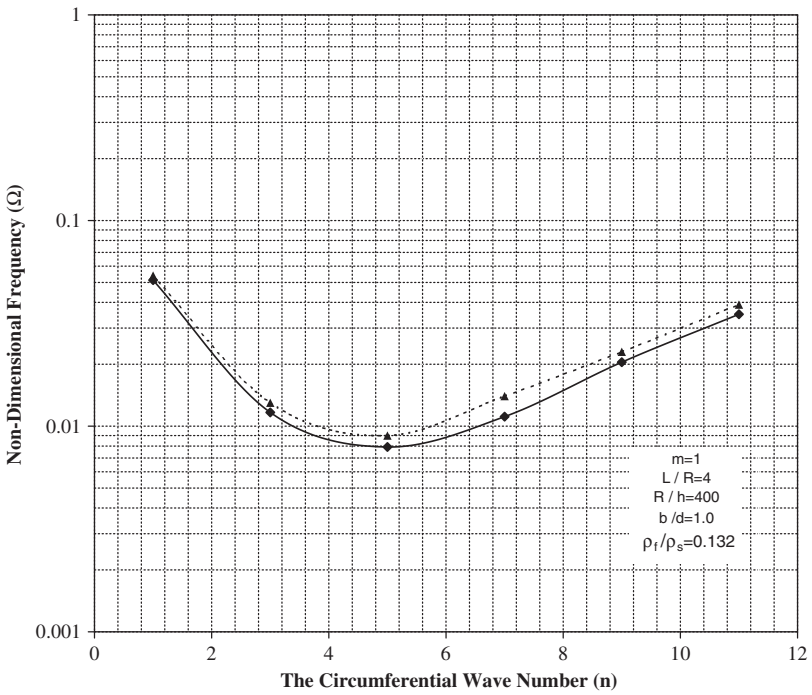

Figure 8. Non-dimensional frequency ($\Omega = \omega R\sqrt{\rho_s(1-\nu^2)/E}$) variation of an immersed cylindrical shell in fluid media.

Table III. Variation of natural frequencies (Hz) of a cylindrical shell with varying eccentricity.

	$e = 0$ mm		$e = 0.5$ mm			$e = 1.0$ mm	
m, n	Reference [19]	Present	Reference [19]	Experiment [19]	Present	Reference [19]	Present
1,2	1340	1330	1347	1330	1335	1302	1294
1,3	3553	3529	3420	3442	3401	3060	2927
1,4	6773	6746	6510	6495	6463	6177	5459
2,2	2105	2050	2071	2063	2043	1955	1905
2,3	3740	3698	3605	3627	3565	3243	3099
2,4	6905	6846	6638	6617	6567	6308	5603
3,2	3598	3517	3542	3463	3469	3302	3205

purely imaginary. The results show that the first loss of stability occurs for $e = 1$ mm. It is concluded that the distortion in the cylindrical shells decreases the critical flow velocity and renders the system less stable.

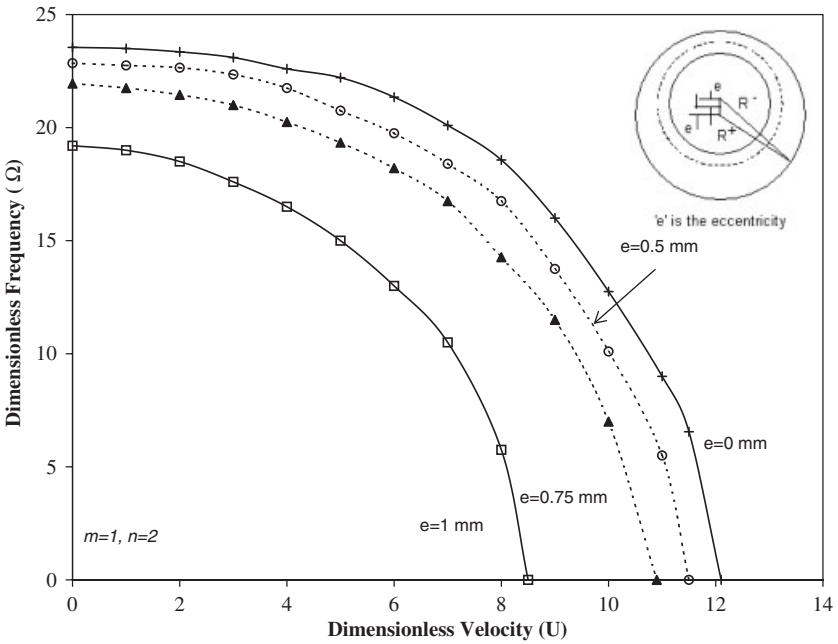

Figure 9. Stability of a distorted cylindrical shell as a function of flow velocity.

7. CONCLUSION

The evaluation of complex vibrational behaviour of the cylindrical tubes, which are subjected to either axial or cross-flow, is highly desirable in different sectors of industry, e.g. nuclear power plants. The study presented in this paper shows an analytical approach that has been developed to study the axially flow-induced vibrations of these structures. An efficient hybrid finite element method, shearable shell theory and linear potential flow have been used to develop the dynamic equations of the coupled fluid–structure system. The shear deformation and rotary inertia effects are taken into consideration. The shells can be uniform or non-uniform in the circumferential direction. The extensional and bending stiffness as well as their coupling have been taken into account.

Some preliminary results show that the effects of rotary inertia are practically limited. Librescu [20] found, in the case of anisotropic plates, that the rotary inertia effect was practically non-existent at least at the lowest branch of the frequency spectrum. The presence of transverse shear deformation effects is very significant and tends to reduce the frequency parameters, especially for laminated anisotropic shells. In general, classical shell theory overestimates frequencies compared to the shear deformation theory, especially for laminated anisotropic shells. It has been suggested that the reason for the difference is a change in shear angle from layer to layer and the insensitivity of Classical Shell Theory (CST) to this change. Following are some conclusions that may be drawn from the obtained results:

(i) The natural frequencies of the coupled fluid–structure are lower than the corresponding values of empty shells, due to increased kinetic energy without a corresponding increase in the strain energy;

(ii) In the case of flowing fluid, the centrifugal and Coriolis terms generate complex eigenvalue problems and non-self-adjoint differential equations; the system may therefore experience static (buckling) and dynamic (flutter) instabilities;
(iii) The shear deformation effect is more pronounced for anisotropic shells and increases with increased shell thickness;
(iv) The frequency reduction of fluid-filled shells becomes more significant as the radius-to-thickness ratio is increased, because the relative increase in kinetic energy due to fluid as compared to that of the shell itself is greater for thinner shells than for thicker shells;
(v) The distortion in the cylindrical shells decreases the critical flow velocity and renders the system less stable.

APPENDIX A

This appendix contains the equations referred to in the various sections of the main text. Matrix $[H]$ elements (Equation (8))

$$
\begin{aligned}
H_{11} &= P_{11}(-\bar{m}^2) - \left[\frac{P_{5,10}+P_{10,5}}{2R^3} - \frac{P_{10,10}}{4R^4} - \frac{P_{55}}{R^2}\right]\eta^2 \\
&\quad - \left[\frac{P_{15}+P_{51}}{R} - \frac{P_{10,1}+P_{1,10}}{2R^2}\right](\bar{m}\eta) \\
H_{12} &= \left(P_{12}+\frac{P_{18}}{2R}\right)(-\bar{m}^2) + \left[\frac{P_{14}+P_{52}}{R} + \frac{P_{58}-P_{10,2}}{2R^2} - \frac{P_{10,8}}{4R^3}\right]\bar{m}\eta \\
&\quad + \left(\frac{P_{54}}{R^2} - \frac{P_{10,4}}{2R^3}\right)\eta^2 \\
H_{13} &= \frac{P_{14}}{R}\bar{m} + \left(\frac{P_{54}}{R^2} - \frac{P_{10,4}}{2R^3}\right)\eta \\
H_{14} &= P_{17}(-\bar{m}^2) - \left[\frac{P_{1,10}+P_{57}}{R} - \frac{P_{10,7}}{2R^2}\right]\bar{m}\eta - \left(\frac{P_{10,10}}{2R^3} - \frac{P_{5,10}}{R^2}\right)\eta^2 \\
H_{15} &= P_{18}(-\bar{m}^2) + \left[\frac{P_{19}+P_{58}}{R} - \frac{P_{10,8}}{2R^2}\right]\bar{m}\eta - \left(\frac{P_{10,9}}{2R^3} - \frac{P_{59}}{R^2}\right)\eta^2 \\
H_{22} &= \left[P_{22} + \frac{P_{28}+P_{82}}{2R} + \frac{P_{88}}{4R^2}\right](-\bar{m}^2) + \left[\frac{P_{24}+P_{42}}{R} + \frac{P_{48}+P_{84}}{2R^2}\right]\bar{m}\eta \\
&\quad - \frac{1}{R^2}(P_{66} - P_{44}\eta^2) \\
H_{23} &= \left(\frac{P_{24}+P_{63}}{R} + \frac{P_{84}}{2R^2}\right)\bar{m} + (P_{44}+P_{66})\frac{\eta}{R^2} \\
H_{24} &= \left(P_{27}+\frac{P_{87}}{2R}\right)(-\bar{m}^2) - \left[\frac{P_{2,10}+P_{47}}{R} + \frac{P_{8,10}}{2R^2}\right]\bar{m}\eta + \frac{\eta^2}{R^2}P_{4,10} + \frac{P_{63}}{R}
\end{aligned}
\tag{A1}
$$

$$H_{25} = \left(P_{28} + \frac{P_{88}}{2R}\right)(-\bar{m}^2) + \left(\frac{P_{29}+P_{48}}{R} + \frac{P_{89}}{2R^2}\right)\bar{m}\eta + \frac{P_{49}}{R^2}\eta^2 + \frac{P_{66}}{R}$$

$$H_{33} = P_{33}(-\bar{m}^2) + \left(\frac{P_{36}+P_{63}}{R}\right)\bar{m}\eta + \frac{P_{66}}{R^2}\eta^2 - \frac{P_{44}}{R^2}$$

$$H_{34} = \left(\frac{P_{47}}{R} - P_{33}\right)(\bar{m}) + \left(\frac{P_{63}}{R} - \frac{P_{4,10}}{R^2}\right)\eta$$

$$H_{35} = \left(P_{36} - \frac{P_{48}}{R}\right)(\bar{m}) + \left(P_{66} - \frac{P_{49}}{R}\right)\frac{\eta}{R}$$

$$H_{44} = P_{77}(-\bar{m}^2) - (P_{7,10} + P_{10,7})\frac{\bar{m}\eta}{R} + \frac{P_{10,10}}{R^2}\eta^2 - P_{33}$$

$$H_{45} = P_{78}(-\bar{m}^2) + (P_{79} + P_{10,8})\frac{\bar{m}\eta}{R} + P_{10,9}\frac{\eta^2}{R^2} - P_{36}$$

$$H_{55} = P_{88}(-\bar{m}^2) + (P_{98} + P_{89})\frac{\bar{m}\eta}{R} + \frac{P_{99}}{R^2}\eta^2 - P_{66}$$

where

$$\bar{m} = \frac{m\pi}{L}$$

The S_f, D_f and G_f terms of Equation (29)

$$\begin{aligned} S_f(i,j) &= -\frac{RL}{2}\Gamma_{ij}(\rho_{fi}Z_{ij} - \rho_{fe}Z_{ej}) \\ D_f(i,j) &= -\frac{m^2\pi^2 R}{2L}\Gamma_{ij}(\rho_{fi}U_{xi}Z_{ij} - \rho_{fe}U_{xe}Z_{ej}) \\ G_f(i,j) &= -\frac{m^2\pi^2 R}{2L}\Gamma_{ij}(\rho_{fi}U_{xi}^2Z_{ij} - \rho_{fe}U_{xe}^2Z_{ej}) \end{aligned} \tag{A2}$$

where $i,j = 1,\ldots,10$, ρ_f is the density of the fluid and subscripts i and e mean, respectively, internal and external flow. The U_x is the velocity of the fluid, Z_{ij} is given in Equation (27) and Γ_{ij} is defined by the following equations:

$$\begin{aligned} \Gamma_{ij} &= \frac{1}{(\eta_i + \eta_j)}[e^{(\eta_i+\eta_j)\varphi} - 1] \quad \text{if } \eta_i + \eta_j \neq 0 \\ \Gamma_{ij} &= \varphi \qquad\qquad\qquad\qquad\quad \text{if } \eta_i + \eta_j = 0 \end{aligned} \tag{A3}$$

where η is the root of the characteristic equation of an empty shell and φ is the angle of each element.

APPENDIX B: NOMENCLATURE

C_{f}	sound speed
f_i	coefficients of the characteristic equation
h	shell thickness
J, Y	Bessel functions of the first and second kind
L	length of the shell
L_i	differential operator of equations of motion
m	axial mode number
$\bar{m} = \dfrac{m\pi}{L}$	
M_{xx}, $M_{x\theta}$, $M_{\theta\theta}$, $M_{\theta x}$	moment resultants
n	circumferential wave number
N_{xx}, $N_{x\theta}$, $N_{\theta\theta}$, $N_{\theta x}$	in-plane force resultants
P_{ij}	terms of elasticity matrix
P_{u}	dynamic pressure
Q_{xx}, $Q_{\theta\theta}$	transverse force resultants
R	mean radius of shell
t	time variable
$U(x,\theta,r,t)$; $V(x,\theta,r,t)$, $W(x,\theta,r,t)$	axial, circumferential and radial displacements respectively,
U_x	axial flow velocity
V_x, V_θ, V_r	axial, circumferential and radial flow velocity, respectively
x	axial coordinate
β_x, β_θ	rotation of tangents to the reference surface
η_i	complex roots of characteristic equation
ε_i	deformation vector components
σ_i	stress vector components
θ	circumferential coordinate
ω	natural frequency
Ω	non-dimensional frequency
ρ_{s}	density of the shell material
ρ_{f}	density of fluid
φ	angle of element
ϕ	potential function

B.1. List of matrices

$\{C\}$	vector of arbitrary constants
$[k_{\mathrm{s}}]$, $[k_{\mathrm{f}}]$	structural and fluid stiffness matrix of an element
$[K_{\mathrm{s}}]$, $[K_{\mathrm{f}}]$	global stiffness matrix of structure and fluid
$[m_{\mathrm{s}}]$, $[m_{\mathrm{f}}]$	structural and fluid mass matrix of an element
$[M_{\mathrm{s}}]$, $[M_{\mathrm{f}}]$	global mass matrix of structures and fluid
$[C_{\mathrm{f}}]$	global damping matrix of fluid
$[N]$	shape function matrix

$[P]$ matrix of elasticity
$[T]$ transformation matrix
$\{\delta_i\}$ degrees of freedom at node i
$\dot{\delta}, \ddot{\delta}$ the first and second time derivative of displacement vector

REFERENCES

1. Païdoussis MP. A review of flow-induced vibrations in reactors and reactor components. *Nuclear Engineering and Design* 1982; **74**(1):31–60.
2. Pettigrew MJ. Flow-induced vibration technology: application to steam generators. *Lecture Series Presented at Babcock & Wilcox Canada*, Canada, 2000.
3. Chen SS. Guidelines for the instability flow velocity of tube arrays in cross-flow. *Journal of Sound and Vibration* 1984; **93**(3):439–455.
4. Weaver DS, Fitzpatrick JA. A review of flow-induced vibrations in heat exchangers. *Proceedings of the First International Conference on Flow-induced Vibrations*. Bowness Windermere, England, 1987; 1–18.
5. Païdoussis MP. *Fluid-structure Interactions, Slender Structures and Axial Flow*, vol. 1. Academic Press: London, 1998.
6. Païdoussis MP. *Fluid-structure Interactions, Slender Structures and Axial Flow*, vol. 2. Academic Press: London, 2003.
7. Pettigrew MJ. Flow-induced vibration phenomenon in nuclear power station components. *Power Industry Research* 1981; **1**:97–133.
8. Seybert AF, Wu TW, Li WL. A coupled FEM BEM for fluid–structure interaction using Ritz vectors and eigenvectors. *Journal of Vibration and Acoustics, Transactions of the ASME* 1993; **115**(2):152–158.
9. Rajasankar J, Iyer NR, Rao T. A new 3-D finite element model to evaluate added mass for analysis of fluid–structure interaction problems. *International Journal for Numerical Methods in Engineering* 1993; **36**(6): 997–1012.
10. Au-Yang MK. *Flow-induced Vibration of Power and Process Plant Components*. ASME Press: New York, 2001.
11. Blevins RD. *Flow-induced Vibration*. Robert E. Krieger Publishing Company Inc.: Malabar, FL, 1990.
12. Saada AS. *Elasticity Theory and Applications*. Pergamon Press: Oxford, 1993.
13. Toorani MH, Lakis AA. General equations of anisotropic plates and shells including transverse shear deformations, rotary inertia and initial curvature effects. *Journal of Sound and Vibration* 2000; **237**(4): 561–615.
14. Sanders JL. An improved first approximation theory for thin shells. *NASA-TR-R24*, 1959.
15. Arnold RN, Warburton GB. Flexural vibration of the walls of thin cylindrical shells having freely supported ends. *Proceedings of the Royal Society of London* 1953; **197A**:238–356.
16. Amabili M, Dalpiaz G. Breathing vibrations of a horizontal circular cylindrical tank shell, partially filled with liquid. *Journal of Vibration and Acoustics* (ASME) 1995; **117**:187–191.
17. Amabili M. Free vibration of partially filled, horizontal cylindrical shells. *Journal of Sound and Vibration* 1996; **191**:757–780.
18. Tonin RF, Bies DA. Free vibration of circular cylinders of variable thickness. *Journal of Sound and Vibration* 1979; **62**(2):165–180.
19. Gonçalve PB, Batista RC. Frequency response of cylindrical shells partially submerged or filled with liquid. *Journal of Sound and Vibration* 1987; **113**(1):59–70.
20. Librescu L. *Elastostatics and Kinetics of Anisotropic and Heterogeneous Shell-type Structures*. Noordhoff International Publishing: Leyden, Netherland, 1975.

